Cyclopamine-paclitaxel-containing nanoparticles: internalization in cells detected by confocal and super-resolution microscopy

(Article begins on next page)

Cyclopamine–Paclitaxel-Containing Nanoparticles: Internalization in Cells Detected by Confocal and Super- Resolution Microscopy

Gaia Fumagalli,[a] Davide Mazza,[b] Michael S. Christodoulou,[a] Giovanna Damia,[c] Francesca Ricci,[c] Dario Perdicchia,[a] Barbara Stella,[d] Franco Dosio,[d] Panagiota A. Sotiropoulou,[e] and Daniele Passarella*[a]

. [a] Dr. G. Fumagalli, Dr. M. S. Christodoulou, Dr. D. Perdicchia, Prof. Dr. D. Passarella Dipartimento di Chimica–Università degli Studi di Milano Via Golgi 19, 20133 Milano (Italy) E-mail: daniele.passarella@unimi.it

. [b] Dr. D. Mazza Centro di Imaging Sperimentale San Raffaele Scientific Institute Via Olgettina 58, 20132 Milano (Italy)

. [c] Dr. G. Damia, Dr. F. Ricci IRCCS-Istituto di Ricerche Farmacologiche Mario Negri Via La Masa 19, 20156 Milano (Italy)

. [d] Dr. B. Stella, Prof. Dr. F. Dosio Dipartimento di Scienza e Tecnologia del Farmaco Università degli Studi di Torino Via Giuria 9, 10125 Torino (Italy)

. [e] Dr. P. A. Sotiropoulou Interdisciplinary Research Institute (IRIBHM) Université Libre de Bruxelles (ULB) 808 Route de Lennik, 1070 Brussels (Belgium)

. Supporting information for this article is available on the WWW under http ://dx.doi.org/10.1002/cplu.201500156.

Abstract

Cyclopamine- and paclitaxel-containing hetero-nanoparticles generated by self-assembly show combined efficacy in the treatment of three different cancer cell lines. The use of ternary combination with the addition of a dye-squalene conjugate secured the obtainment of fluorescent nanoparticles that permit-ted the observation of the cellular internalization by confocal microscopy and super-resolution dSTORM (direct stochastic optical reconstruction microscopy).

Tumors are heterogeneous, composed of distinct types of cells including cancer stem cells (CSCs), which exhibit high clono- genic capacity and the ability to reform parental tumors upon transplantation. Existing anticancer therapies are in most cases palliative rather than curative, not being able to prevent re- lapse. One possible explanation is that current treatments target the more differentiated tumor cells resulting in tumor regression; they do not target CSCs, and subsequently there is a relapse of the disease. Indeed, resistance to therapy has been shown for several types of CSCs. Therefore, a combination of agents against both CSCs and bulk tumor cells may offer improved therapeutic benefits.[1] In this field, the use of a combination of paclitaxel, a known microtubule stabilizer, and cyclopamine, a natural alkaloid acting as Hedgehog signalling pathway (Hh) inhibitor, has been reported for the treatment of some prostate cancer cells resulting in decreased proliferation and increased apoptosis.[2,3]

The use of nanotechnology can overcome some problems of drug delivery[4–10] improving the cell internalization of other- wise insoluble, unstable, or unavailable therapeutic com- pounds and reducing the dosage of those compounds and the associated side effects.[11] In this light, we recently described the preparation of a novel class of squalene-based releasable compounds conjugated with paclitaxel, podophyllotoxin, camptothecin, and epothilone A. Owing to the presence of the squalene tail and the disulfide-containing linker, the derivatives self-assembled in water to form nanoparticles and the drug was released after cell internalization[12] as a possible consequence of the presence of glutathione (GSH). Couvreur et al. reported the possibility to obtain self-assembled fluorescent hetero-nanoparticles.[13] In our case, we recently described the combination of paclitaxel–squalene and fluoresceine–squalene conjugates to trace the delivery of the nanoassemblies and to investigate the internalization mechanism.[14]

Following our interest in the synthesis and functionalization of new anticancer compounds,[15–21] we examine self-assembled hetero-nanoparticles that incorporate two different drugs: paclitaxel and cyclopamine (1a). A ternary combination obtained by further addition of a tetramethylrhodamine–

squalene conjugate generated fluorescent nanoparticles that could be used to observe the cellular internalization by confocal microscopy and super-resolution dSTORM.[22]

We first investigated the synthesis of cyclopamine–squalene conjugates incorporating a disulfide bond. In Scheme 1 we report a successful synthesis that relies on the protection of the amino group.[4] Condensation of cyclopamine N-Fmoc (1b)[23] with dicarboxylic acid monoesters 2a,b[12] in the presence of EDC–DMAP and subsequent removal of the protecting group led to cyclopamine conjugates 3a,b.The conjugates ob- tained were used to form nanoparticles by the solvent-dis- placement method which were characterized by quasi elastic light scattering (QELS) (Table 1).

To assess the effect of the compounds 3 a and 3 b on cancer cell growth, we evaluated their biological effect in U251 glioblastoma cell line taking into account that their resistance is associated also with an increase of GSH level.[24] We found compound 3 b to be the more active (Figure S1 in the Support- ing Information). Our results show that the compound 3 b inhibited proliferation (Table 1) and induced apoptosis at comparable levels to that of cyclopamine, and this effect was indeed mediated by inhibition of the Hh pathway (Figure S1 in the Supporting Information). In our proposal, compound 3 a releases the drug as a consequence of the cleavage of the disulfide bond by glutathione (GSH), which is particularly present inside the cancer cells. If the release of cyclopamine is responsible for the activity, the unexpected result seems to suggest a better release in compound 3 b. With the aim to evaluate the chemical reactivity induced by the presence or the absence of the disulfide bond, we studied the behavior of both compounds 3a and 3b in the presence of GSH. With ESI mass spectrometry we had the possibility of detecting the release of cyclopamine from both of the compounds. In the absence of GSH we observed only the peaks of the conjugate (see the Supporting In- formation).

Given the better activity of compound3b, we decided to use compound 3 b and compound 4[12] to form hetero-nanoparticles. Hetero-nanoparticles having different molar ratios of the two compounds were prepared; the results obtained with the most active nanosuspension (molar ratio 3 b/4 23 :1). Hetero-nanoparticles were characterized using QELS (Table 1) and the morphology was evaluated by AFM (Figure 1). Biological evaluation of hetero-nanoparticles (Table 1) showed that the activity of the two drugs was maintained and comparable to the activity of nanoassemblies of compounds 3 b and 4 in different cellular systems, that is, OVCAR5 (ovarian cancer cell) and #83 and #110 (ovarian tumor- initiating cells).[25] The inhibition of U251 proliferation (Figure S2 in the Supporting Information) and

induction of apoptosis (Figure 2) showed a combined effect. It is worth noting that the IC_{50} value reported for 3b/4 NPs refers to sum of the concentrations of the two compounds assembled in the hetero-nanoparticles: this means that for the reported values 23/24 is due to compound 3 b and 1/24 to compound 4. As an example, the IC_{50} obtained for 3 b/4 in U251 cells corresponds to a concentration of compound 4 equal to 1.2 mm and to a concentration of compound 3 b equal to 26.8 mm, both lower than the IC_{50} obtained for the corresponding homo-nanoparticles.

Next, we aimed to monitor the ability of the hetero-nanoparticles to pass through the cell membrane in biological media. In order to apply fluorescence microscopy, we assembled hetero-NPs that incorporated a squalene–tetramethylrhodamine (TAMRA) conjugate (6). TAMRA was chosen as a fluorescent dye because it is used in super-resolution localization microscopy techniques such as dSTORM (direct stochastic optical reconstruction microscopy).[26] The fluorescent squalene conjugate was synthesized by reaction of tetramethylrhodamine isothiocyanate (5) with compound 7[12] in the presence of sodium hydride (Scheme 2). The fluorescent hetero-nanoparticles were obtained by the solvent-displacement method by mixing compounds 3 b, 4, and 6 in a 23 :1:15 molar ratio ; we confirmed by QELS the formation of the nanoparticles [mean diameter : (224 2) nm, zeta potential : (+ 43.5 3.4) mV] .

Breast cancer MCF-7 cells were treated with the fluorescent hetero-nanoparticles for 20 min and imaged by multiple fluorescence microscopy methods. Three-dimensional confocal microscopy (Figure 3) allowed the identification of the fluorescent nanoparticles in the cytoplasm of the cells, providing evi- dence that the nanoparticles are capable of permeating the cellular membrane. However, to provide an estimation of the size of the NPs, the resolution of conventional microscopy is not sufficient. We therefore applied super-resolution microscopy (dSTORM)[27] to quantify the diameter of the bright particles detected inside the cells. Figure 4 shows images of the cells re- corded after 1.5 h of incubation. The enlarged detail of the NP served to quantify its diameter : 156 nm. The diameter is in good agreement with our previous measurements by QELS [(224 2) nm] . In order to monitor the behavior of the internalized NPs, we performed dStorm imaging at different incubation times. In this way we confirmed (Table 2) a progressive in- crease in the variability of the nanoparticle diameter—as indicated by the increase in the coefficient of variation—which might be an indication of their tendency to disassemble.

In conclusion, we have demonstrated the possibility of forming hetero-nanoparticles containing two different drugs and we also established that the two drugs that do not influence each other's activity. We confirmed the possibility of following the internalization mechanism by the addition of a third dye-based compound using super-resolution microscopy. Our approach is based on simple chemical functionalization of known anticancer compounds that self-assemble to form nanoparticles. In principle, this could improve drug biocompatibility and delivery efficacy. In this specific study the discussed approach yielded results that may be useful in overcoming resistance due to cancer stem cells. We consider that the functionalization of different known drugs with a cleavable linker and a proper lipophilic chain that induces self-assembly and the generation of hetero-nanoparticles could be exploited for personalized treatment of different types of diseases, and it may be possible to trace these nanoparticles in the cells by imaging.

Acknowledgements

. [1] P. A. Sotiropoulou, M. S. Christodoulou, A. Silvani, C. Herold-Mende, D. Passarella, Drug Discovery Today 2014, 19, 1547–1562.

. [2] Y. Zhou, J. Yang, J. S. Rhim, J. Kopecˇek, J. Controlled Release 2013, 172, 946 – 953.

. [3] S. Singh, D. Chitkara, R. Mehrazin, S. W. Behrman, R. W. Wake, R. I. Mahato, PLoS One 2012, 7, e40021.

. [4] H. Hillaireau, P. Couvreur, Cell. Mol. Life Sci. 2009, 66, 2873–2896.

. [5] P. Couvreur, C. Vauthier, Pharm. Res. 2006, 23, 1417–1450.

. [6] P. Couvreur, B. Stella, L. H. Reddy, S. Mangenot, J. H. Poupaert, D. Des- maele, S. Lepetre-Mouelhi, F. Rocco, N. Dereuddre-Bosquet, P. Clayette, V. Rosilio, V. Marsaud, J. M. Renoir, L. Cattel, Nano Lett. 2006, 6, 2544 – 2548.

. [7] D. Desma le, R. Gref, P. Couvreur, J. Controlled Release 2012, 161, 609– 618.

. [8] N. SØmiramoth, C. Di Meo, F. Zouhiri, F. Sa ̈id-Hassane, S. Valetti, R. Gorges, V. Nicolas, J. H. Poupaert, S. Chollet-Martin, D. Desmaele, R. Gref, P. Couvreur, ACS Nano 2012, 6, 3820– 3831.

. [9] F. Dosio, L. H. Reddy, A. Ferrero, B. Stella, L. Cattel, P. Couvreur, Bioconju- gate Chem. 2010, 21, 1349–1361.

. [10] J. Caron, A. Maksimenko, S. Wack, E. Lepeltier, C. Bourgaux, E. Morvan, K. Leblanc, P. Couvreur, D. Desmaele, Adv. Healthcare Mater. 2013, 2, 172 – 185.

[11] D. A. LaVan, T. McGuire, R. Langer, Nat. Biotechnol. 2003, 21, 1184 – 1191.

. [12] S. Borrelli, M. S. Christodoulou, I. Ficarra, A. Silvani, G. Cappelletti, D. Car- telli, G. Damia, F. Ricci, M. Zucchetti, F. Dosio, D. Passarella, Eur. J. Med. Chem. 2014, 85, 179.

. [13] D. T. Bui, J. Nicolas, A. Maksimenko, D. Desma le, P. Couvreur, Chem. Commun. 2014, 50, 5336–5338.

. [14] S. Borrelli, D. Cartelli, F. Secundo, G. Fumagalli, M. S. Christodoulou, A. Borroni, D. Perdicchia, F. Dosio, P. Milla, G. Cappelletti, D. Passarella, ChemPlusChem 2015, 80, 47–49.

. [15] F. Calogero, S. Borrelli, G. Speciale, M. S. Christodoulou, D. Cartelli, D. Ballinari, F. Sola, C. Albanese, A. Ciavolella, D. Passarella, G. Cappelletti,

S. Pieraccini, M. Sironi, ChemPlusChem 2013, 78, 663 – 669.

. [16] E. Riva, M. Mattarella, S. Borrelli, M. S. Christodoulou, D. Cartelli, M. Main, S. Faulkner, D. Sykes, G. Cappelletti, J. S. Snaith, D. Passarella, ChemPlusChem 2013, 78, 222–226.

. [17] M. S. Christodoulou, F. Zunino, V. Zuco, S. Borrelli, D. Comi, G. Fontana, M. Martinelli, J. B. Lorens, L. Evensen, M. Sironi, S. Pieraccini, L. Dalla Via, O. M. Gia, D. Passarella,

ChemMedChem 2012, 7, 2134 – 2143.

.   [18] C. Peruzzotti, S. Borrelli, M. Ventura, R. Pantano, G. Fumagalli, M. S. Christodoulou, D. Monticelli, M. Luzzani, A. L. Fallacara, C. Tintori, M. Botta, D. Passarella, ACS Med. Chem. Lett. 2013, 4, 274–277.

.   [19] F. Arioli, S. Borrelli, F. Colombo, F. Falchi, I. Filippi, E. Crespan, A. Naldini, G. Scalia, A. Silvani, G. Maga, F. Carraro, M. Botta, D. Passarella, Chem- MedChem 2011, 6, 2009–2018.

.   [20] M. S. Christodoulou, N. Fokialakis, D. Passarella, A. N. García-Argµez, O.M. Gia, I. Pongratz, L. DallaVia, S.A. Haroutounian, Bioorg. Med. Chem. 2013, 21, 4120–4131.

.   [21] M. S. Christodoulou, F. Colombo, D. Passarella, G. Ieronimo, V. Zuco, M. De Cesare, F. Zunino, Bioorg. Med. Chem. 2011, 19, 1649 – 1657.

.   [22] D. R. Whelan, T. Holm, M. Sauer, T. D. M. Bell, Aust. J. Chem. 2014, 67, 179 – 183

.   [23] M. R. Tremblay, M. Nevalainen, S. J. Nair, J. R. Porter, A. C. Castro, M. L. Behnke, L. C. Yu, M. Hagel, K. White, K. Faia, L. Grenier, M. J. Campbell, C. N. Cushing, C. N. Woodward, J. Hoyt, M. A. Foley, M. A. Read, J. R. Sydor, J. K. Tong, V. J. Palombella, K. McGroven, J. Adams, J. Med. Chem. 2008, 51, 6646–6649.

.   [24] F. Ricci, S. Bernasconi, P. Perego, M. Ganzinelli, G. Russo, F. Bono, C. Man- gioni, R. Fruscio, M. Signorelli, M. Broggini, G. Damia, Cell Cycle 2012, 11, 1966–1976.

.   [25] C. R. Oliva, D. R. Moellering, G. Y. Gillespie, C. E. Griguer, PLoS One 2011, 6, e24665.

.   [26] M. Heilemann, S. Van De Linde, A. Mukherjee, M. Sauer, Angew. Chem. Int. Ed. 2009, 48, 6903–6908; Angew. Chem. 2009, 121, 7036–7041.

.   [27] T. Klein, A. Lçschberger, S. Proppert, S. Wolter, S. Van De Linde, M. Sauer, Nat. Methods 2011, 8, 7–9.
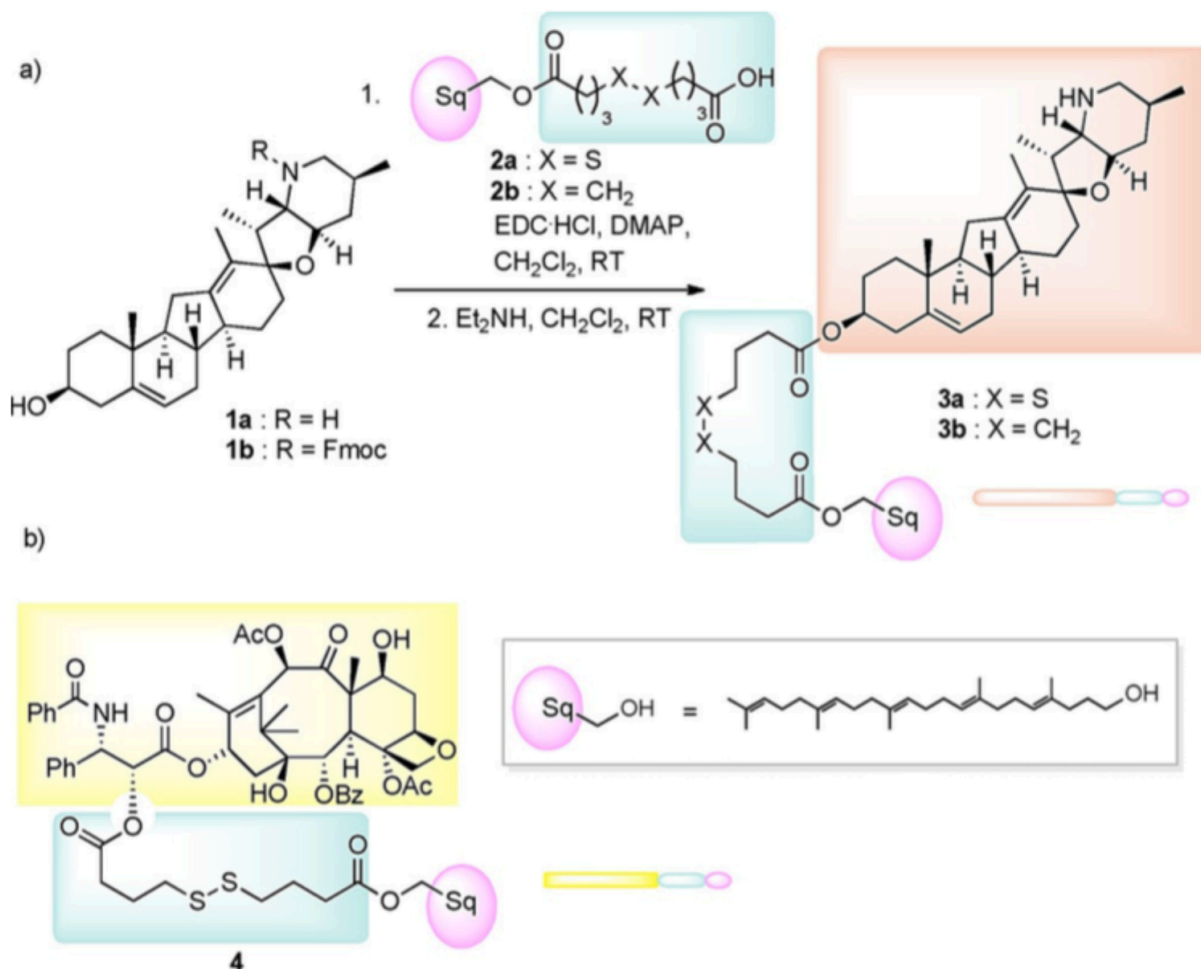
Scheme 1. a) Synthesis of the cyclopamine conjugates 3 a,b; b) Structure of paclitaxel–squalene derivative 4. EDC=N-(3-dimethylaminopropyl)-N′-ethyl-carbodiimide hydrochloride, DMAP=4-(dimethylamino)pyridine, Fmoc=9-fluorenylmethoxycarbonyl.

Scheme 2. Synthesis of the fluorescent squalene conjugate.

Table 1. Mean diameter of NPs, zeta potentials, and the IC_{50} values determined with different cell lines.

Compound	Diameter[a] [nm]	Zeta potential [mV]	#83	#110	OVCAR5	U251
				IC_{50} [μM]		
1a	–	–	>50	>50	>50	30
3a (NP)	105±1	+37.8±3.3	n.a.[b]	n.a.[b]	n.a.[b]	68
3b (NP)	240±2	+38.4±4.3	34	40	42	40
4 (NP)	437±5	−35.7±0.1	<3	<3	<3	4
3b/4 (NP)[c]	229±2	+26.4±1.7	16	15	32	28

[a] Mean diameter. [b] Not available. [c] Molar ratio **3b/4**=23:1.

Table 2. Mean diameter of three-component hetero-NPs (**3a/4/6**= 23:1:15) at different times after the incubation.

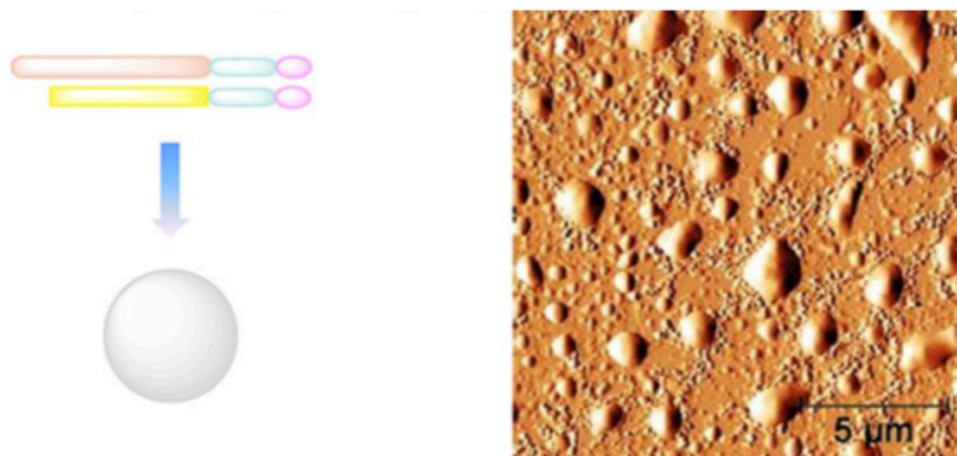| Time after incubation [h]	Mean diameter [nm]	Coefficient of variation	Number of cells
0.5	147±17	0.12	10
1	140±31	0.22	10
1.5	178±63	0.36	12

Figure 1. AFM picture showing the morphology of **3b/4** hetero-nanoparticles (molar ratio 23:1).
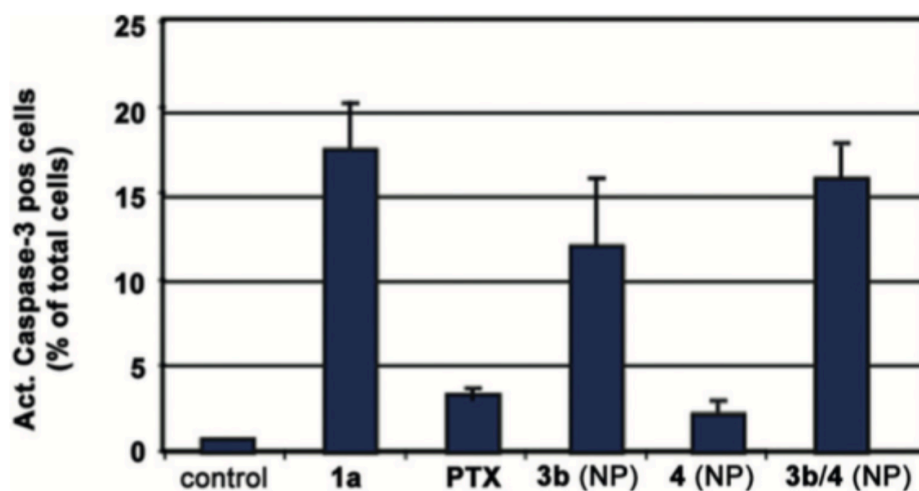

Figure 2. Apoptosis of the U251 glioblastoma cell line, expressed as percentage of total cells expressing active caspase-3, 24 h upon addition of the mentioned compounds; **1a**: 2.07 μM; PTX (paclitaxel): 0.094 μM; **3b** (NP): 2.07 μM; **4** (NP): 0.094 μM; **3b/4** (NP): 2.07 μM/0.094 μM.
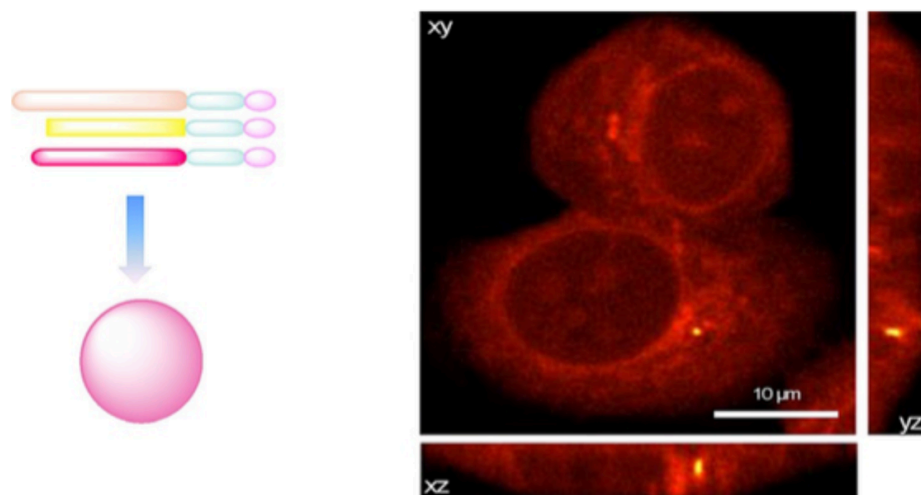
Figure 3. Cellular imaging of three-component **3b/4/6** hetero-NPs. Confocal imaging of cells treated for 20 min with fluorescent hetero-nanoparticles. Displayed are the orthogonal projection of the three-dimensional stack for two MCF-7 cells. The bottom cell shows a bright fluorescent dot (a putative hetero-NP) in the cytoplasmplasm close to the nucleus.
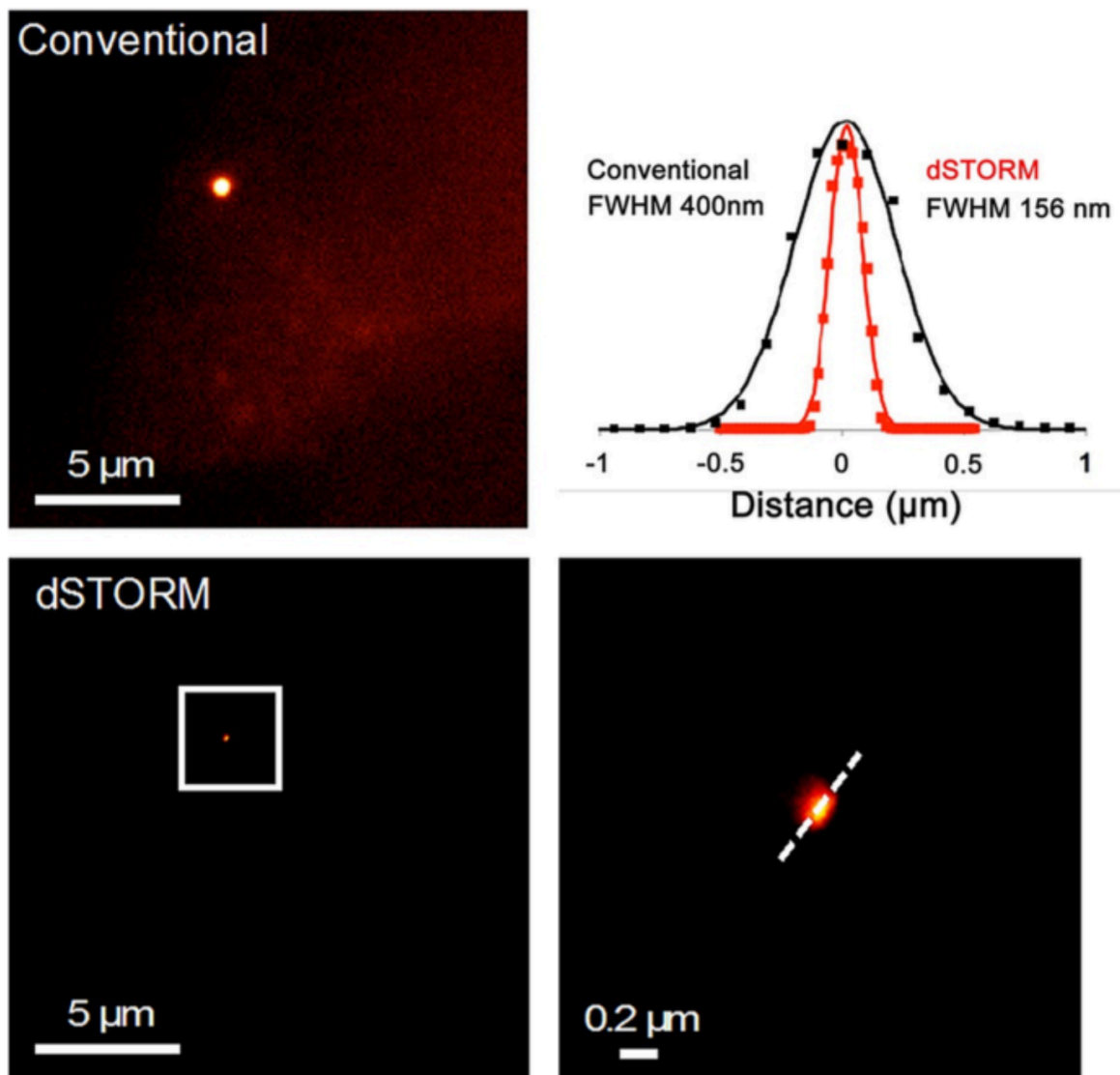
Figure 4. Cellular imaging of three-component hetero-NPs. Results obtained from application of super-resolution dSTORM: shown are the conventional widefield image (top left) and the super-resolution image (bottom left) of the same cell together with a enlarged detail of the NP (bottom right) and the quantification of the diameter of the shown NP in the conventional and the super-resolution image (top right). FWHM=full width at half maximum.